The Generation of Diurnal Period Shelf Waves by Tidal Currents

RICHARD E. THOMSON AND WILLIAM R. CRAWFORD

Department of Fisheries and Oceans, Institute of Ocean Sciences, Sidney, British Columbia V8L 4B2 Canada

(Manuscript received 18 December 1981, in final form 17 March 1982)

ABSTRACT

Continental shelf waves of diurnal period are shown to be generated by tidally induced Reynolds stresses within a bottom Stokes-scale boundary layer. The theory is applicable to a uniformly rotating, homogeneous ocean of two-dimensional depth variability in which alongshore variations occur over scales large compared to the shelf width. Explicit solutions are derived for the shelf wave velocity components and for the cross-shelf sea surface slope in the case of a traveling Kelvin wave forcing. Numerical values are presented for an exponential depth profile $H = H_0 \exp(-2\alpha x)$, where x is the coordinate normal to the coast. Results indicate that the amplitude of the shelf wave current can exceed that of the astronomical tidal current and that the alongshore component of the shelf wave current will consistently lead the alongshore component of the tidal current by 180° to 0° over one wavelength in the direction of phase propagation.

1. Introduction

Continental shelf waves with periods of days and wavelengths of hundreds of kilometers are commonly observed features of coastal oceanic regions. Generated by transient wind systems, these low-frequency current and sea level oscillations have been the focus of considerable theoretical and observational research within the last decade and a half (e.g., Allen, 1980; Mysak, 1980). Shelf waves of tidal diurnal periods, on the other hand, have received comparatively little attention despite the fact that their existence was established as early as 1969 (Cartwright, 1969).

Two principal reasons can be cited for the paucity of data on diurnal continental shelf waves. First, the fluid motions associated with the waves are accurately detected only by current meter and cross-shelf sea level measurements. Second, and perhaps more important, the waves are confined to limited extents of mid-to-high latitude coasts where the restoring mechanism provided by the bottom topography is capable of supporting such relatively high-frequency, subinertial oscillations. This contrasts with low-frequency shelf waves for which the topographic restoring is not generally a limiting factor to the motions.

Shelf waves of predominantly K_1 and O_1 tidal frequency were first observed in current meter records from the shelf region of the outer Hebrides off western Scotland (Cartwright, 1969; Cartwright *et al.*, 1980). Currents associated with the waves are found to be barotropic and to have amplitudes comparable to the accompanying diurnal tidal flows. The shelf waves appear to be restricted to first mode oscillations in approximate anti-phase to the tidal motions, where the latter have the form of northward propagating barotropic Kelvin waves. More recent evidence for diurnal shelf waves has been obtained from current meter and sea level records collected in 1979–80 during the Coastal Oceanic Dynamics Experiment (CODE) off the west coast of Vancouver Island, British Columbia (Crawford and Thomson, 1982). As with previous observations, the shelf waves occur as first mode quasi-barotropic fluctuations at the K_1 and O_1 tidal frequencies. Off Vancouver Island, these waves result in an approximate five-to-ten-fold amplification of the diurnal currents on the shelf compared to the adjacent deep-sea region as well as to marked alongshore and across-shore variations in the tide-current phases. Such motions are not, however, observed south of the Washington coast or north of Vancouver Island (e.g., Thomson and Huggett, 1981).

The purpose of this paper is to show that shelf waves can be generated by tidal motions over the shelf regions of continental margins. Particular attention is given waves of diurnal frequency although the analysis applies equally well to oscillations at other subinertial tidal frequencies. It is shown that diurnal shelf waves occur in response to the alongshore component of the bottom Reynolds stress associated with a tidally induced time-dependent boundary layer. The forcing mechanism exists everywhere there are significant diurnal tides, whereas the response is limited to sections of a coast having sufficiently broad shelves or steep slopes to support first mode diurnal shelf wave oscillations. To accommodate this aspect of the generation, our analysis permits a slow alongshore variation in the depth such

0022-3670/82/070635-09$06.25

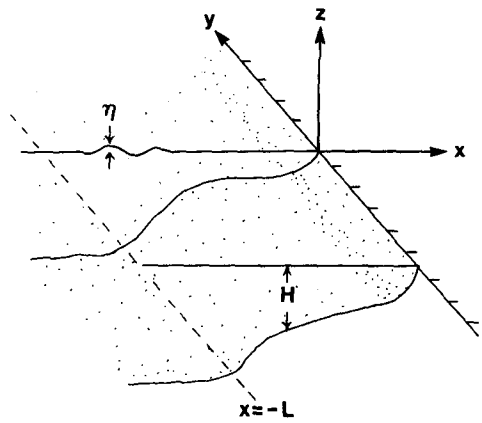

FIG. 1. Coordinate system.

that for a given tidal frequency there is an initial location where the forced shelf waves are first possible. In many respects, the following analysis represents a generalized version of the one used successfully by Gill and Schumann (1974) to describe wind-generated continental shelf waves.

2. The vorticity equation

We consider a uniformly rotating, homogeneous ocean of variable depth $H(x, y)$ and shelf width $L(y)$ bordered by a straight coastline and occupying the semi-infinite region $x \leq 0, -\infty < y < \infty, z \leq 0$ (Fig. 1). Surface winds are omitted and the ocean is assumed to be frictionless except for a thin, Ekman-type bottom boundary layer. Within the bulk of the fluid, motions are expressed in terms of depth-independent barotropic modes with horizontal velocity components, i.e.,

$$(U, V) = H^{-1} \int_{-H}^{0} (u, v) dz, \qquad (2.1)$$

defined here as depth-averaged values of the instantaneous velocity components (u, v).

The barotropic motions (2.1) are assumed to be a superposition of planetary-scale Kelvin waves and mesoscale continental shelf waves coupled only through near-bottom Reynolds stresses. The Kelvin waves represent the astronomical tides in the present context and are, of course, ubiquitous features of the ocean basin. They span a broad range of frequencies, both superinertial and subinertial, and because of their large scales are little affected by the detailed bathymetry of the continental margin. The existence of these waves is implicit in our analysis. Continental shelf waves, on the other hand, are necessarily of subinertial frequency, with the range of frequencies attainable by a particular mode strongly determined by the shelf-slope topography. An important assumption to be made later in the analysis is that shelf waves within the frequency band of interest are possible only for a limited section of the coast.

If we make the Boussinesq and hydrostatic approximations, the equations of momentum and mass conservation for long barotropic waves can be written as

$$(U_t - fV + g\eta_x) = -H^{-1}\tau^{(x)}, \qquad (2.2)$$

$$(V_t + fU + g\eta_y) = -H^{-1}\tau^{(y)}, \qquad (2.3)$$

$$(UH)_x + (VH)_y + \eta_t = 0, \qquad (2.4)$$

where ρ_0 is a constant reference density, f the vertical component of the earth's rotation, g gravity, η the sea-surface displacement, t the time, and $\tau^{(x,y)}$ are the (x, y) components of the bottom Reynolds stress. Provided the length scale L of the shelf waves is considerably less than the external radius of deformation (i.e., $f^2L^2/gH \ll 1$), as is usually the case off mid-to-high latitude coastlines, the customary rigid lid assumption can also be made (cf., LeBlond and Mysak, 1978). Because this eliminates long gravity waves from the equations, we can ignore η_t in (2.4) and define a transport streamfunction ψ by

$$UH = \psi_y, \quad VH = -\psi_x. \qquad (2.5)$$

Combining (2.5) with cross differentiation of (2.2) and (2.3) and the requirement that alongshore scales $\hat{L}$ significantly exceed cross-shelf scales L (i.e., $\partial/\partial y \ll \partial/\partial x$), we obtain the vorticity equation

$$\rho_0 H(H^{-1}\psi_x)_{xt} + \rho_0 f H^{-1}(H_x\psi_y - H_y\psi_x) = -H^{-1}H_x\tau^{(y)}. \qquad (2.6)$$

This equation is correct to order $\epsilon^2 = (L/\hat{L})^2 \ll 1$ and is subject to the boundary conditions

$$\psi = O(HU = 0) \quad \text{at} \quad x = 0, \qquad (2.7a)$$

$$\psi_x = O(V = 0) \quad \text{at} \quad x = -L. \qquad (2.7b)$$

Two additional assumptions used in the derivation of (2.6) are that ω/f is of order ϵ (ω is the wave frequency) and that the forcing term $\tau_x^{(y)} \ll (H_x/H)\tau^{(y)}$. For diurnal frequency motions $\epsilon \approx 0.6$, so that the former assumption severely restricts the validity of our perturbation expansion. However, from a practical point of view, it is necessary if we are to obtain analytical solutions to the vorticity equation. The latter assumption, in contrast, is readily justified provided that bottom stress is linked to the large scale Kelvin wave (tidal) motions.

A straightforward, linear model for the alongshore component of the Reynolds stress is

$$\tau^{(y)} = \rho_0 \mu v_z \approx \rho_0 \mu \delta^{-1} v_0, \qquad (2.8)$$

in which μ is a constant vertical eddy viscosity, $\delta = (2\mu/\omega)^{1/2}$ is the thickness of the time-dependent bottom boundary layer (Batchelor, 1967), and v_0 is the alongshore component of the tidal current at the top of the boundary layer. Substitution of (2.8) into

(2.6) then yields the forced vorticity equation

$$f^{-1}H(H^{-1}\psi_x)_{xt} + H^{-1}(H_x\psi_y - H_y\psi_x) = -\mathrm{E}^{1/2}(\omega H_0/fH)H_x v_0\,, \quad (2.9)$$

where

$$\mathrm{E} = \mu/(2\omega H_0^2) \quad (2.10)$$

is an Ekman-type number and H_0 is a scale depth for the continental shelf region. The form of (2.9) is unchanged following nondimensionalization and implies that the magnitude of the alongshore forcing is of order $\mathrm{E}^{1/2}$. However, the magnitude of the force can be expected to vary considerably in the cross-shelf direction, ranging from near-zero values in offshore regions to relative maxima just seaward of the shelf break and near the coast where $(H_0/H)H_x v_0$ is comparatively large.

3. Solution of the vorticity equation

Separable solutions to (2.9) are possible if the scale heights of alongshore depth changes are of order ϵH or if the alongshore length scale $\hat{L}$ for depth variations is of order $\epsilon^2 L$. We consider the latter to be the case and transform to the two variables

$$y = y, \quad \tilde{y} = \epsilon y, \quad (3.1)$$

defined as the "fast" and "slow" variables, respectively. The depth is therefore of the form

$$H = H(x, \tilde{y}). \quad (3.2)$$

Following Gill and Schumann (1974) we next expand the streamfunction ψ and alongshore component of the tidal velocity v_0 in the cross-shelf eigenfunctions ϕ_n of the free-wave problem ($v_0 \equiv 0$). In terms of the two alongshore variables (3.1), the streamfunction becomes

$$\psi(x, y, t) = \sum_{n=1}^{\infty} \{\Psi_{0n}(y, \tilde{y}, t) + \epsilon\Psi_{1n}(y, \tilde{y}, t) + \cdots\}\phi_n(x, \tilde{y}), \quad (3.3)$$

where n is the cross-shelf mode number. To expand v_0, we use the fact that the length scale $(gH)^{1/2}f^{-1}$ of barotropic Kelvin waves greatly exceeds the shelf width, so that v_0 can be considered to be independent of x. This leads to the equation

$$1 = \sum_{n=1}^{\infty} b_n(\tilde{y})\phi_n(x, \tilde{y}), \quad (3.4)$$

whose physical interpretation has been given by Gill and Schumann in terms of the expansion of the Ekman transport in the surface boundary layer. In the present case, the bottom Ekman transport satisfies

$$\tau^{(y)}/\rho_0 f \sim \mathrm{E}^{1/2}(\omega/f)H_0^2 v_0\,,$$

which, according to (3.4) is uniform in the offshore region except for a discontinuity at the coast ($x = 0$) where $\phi_n(x)$ vanishes.

Substitution of (3.3) into (2.9), combined with boundary conditions (2.7a,b), gives the well-known Sturm-Liouville eigenvalue problem for the cross-shelf structure of the streamfunction:

$$(H^{-1}\phi_{n,x})_x - f(c_{0n}H)^{-1}H_x\phi_n = 0, \quad (3.5)$$

$$\phi_n = 0 \quad \text{at} \quad x = 0, \quad (3.6a)$$

$$\phi_{n,x} = 0 \quad \text{at} \quad x = -L, \quad (3.6b)$$

where $c_{0n}(\tilde{y})$ is the separation variable. Although analytical solutions to these equations can be derived for certain idealized forms of bottom topography (e.g., Mysak, 1980), solutions for a specific continental margin usually must be obtained through numerical integration.

The alongshore structure of the streamfunction is determined by a set of first order wave equations in (y, t). To orders ϵ^0 and ϵ^1 these are, respectively,

$$(c_{0n})^{-1}\Psi_{0n,t} + \Psi_{0n,y} = -\mathrm{E}^{1/2}(\omega/f)H_0 b_n v_0\,, \quad (3.7)$$

$$(c_{1n})^{-1}\Psi_{1n,t} + \Psi_{1n,y} = \sum_{m=1}^{\infty} d_{mn}\Psi_{0m}\,. \quad (3.8)$$

The coefficient b_n in (3.7) is obtained from (3.4) using the orthogonality condition for ϕ_n (Morse and Feshbach 1953, p. 727);

$$\int_{-L}^{0} H^{-2}H_x\phi_n\phi_m dx = -\delta_{mn}\,, \quad (3.9)$$

where δ_{nm} is the Kronecker delta. This yields

$$b_n(\tilde{y}) = -\int_{-L}^{0} H^{-2}H_x\phi_n dx. \quad (3.10)$$

Similarly, use of the orthogonality conditions yields

$$d_{mn}(\tilde{y}) = -H^{-2}\int_{-L}^{0} H_{\tilde{y}}\Psi_{0n}\phi_{n,x}\phi_{m,x}dx - \Psi_{0n,\tilde{y}} \quad (3.11)$$

for the coefficient in (3.8).

The solution of (3.7) and (3.8) follow the same general procedure so we confine our attention to the zeroth order equation only. With the transformation of variables $(y, t) \rightarrow (\eta, \xi)$, where

$$\eta = y, \quad \xi = \int dy/c_{0n} - t,$$

Eq. (3.7) takes the form

$$\Psi_{0n,\eta} = -\mathrm{E}^{1/2}(\omega/f)H_0 b_n v_0\,. \quad (3.12)$$

Definitive solutions to (3.12) can be derived by integration along the characteristic

$$\xi = \text{constant} = \int^{y} dy/c_{0n} - t$$

provided that the onset time or starting location of

the waves is known. The direction of integration must be consistent with the fact that shelf waves propagate with the coast to the right in the Northern Hemisphere and to the left in the Southern Hemisphere. In this paper, we are assuming that there is a finite length only of any given coastline where the topographic restoring mechanism can support shelf wave fluctuations of frequency ω. Hence, we begin integration of (3.12) in the direction of phase propagation from the initial alongshore location $\eta = y_0$ where shelf waves at this particular frequency are first possible. Taking $\Psi_{0n} = 0$ at this point, we obtain the zeroth order value of Ψ at another location y at time t as

$$\Psi_{0n}(y, t) = -E^{1/2}(\omega/f)H_0 b_n \int_{y_0}^{y} v_0(\eta, s + t)d\eta, \quad (3.13)$$

in which b_n is defined by (3.9) and

$$s(\eta, y) = \int_{y}^{\eta} c_{0n}^{-1} dy. \quad (3.14)$$

4. Response to a traveling Kelvin wave forcing

a. The streamfunction

To obtain explicit expressions for the streamfunction (3.3), both the cross-shore and alongshore components must be separately determined. The eigenfunctions ϕ_n and corresponding eigenvalues c_{0n} for a particular oceanic region of depth $H(x, \tilde{y})$ can be obtained analytically or by numerical integration of (3.5) using boundary conditions (3.6). The latter lead, in turn, to the dispersion relation $\omega_n(k_n)$ for alongshore wavenumber k_n, with frequency decreasing with mode number (n) for a given wavenumber. Shelf waves are observed to be confined to the first few modes and typically to have frequencies well below the diurnal frequency band. Observed properties of shelf waves and analytical details for determination of their cross-shelf structure have been reviewed by Mysak (1980), Allen (1980) and Huthnance (1981) and need not be repeated here. The reader is referred to Cartwright *et al.* (1980) and Crawford and Thomson (1982) for details regarding the shelf wave structure off the coasts of the Hebrides and Vancouver Island, respectively.

We now wish to deal specifically with the generation and alongshore structure of diurnal shelf waves. To do this we take an oceanic region where the coastal bathymetry is capable of supporting such waves and where the cross-shelf wave structure is described by the eigenfunction solution to (3.5) and (3.6). Moreover, we need only consider the lowest mode ($n = 1$) wave since it appears, on the basis of realistic depth profiles, that this mode alone can attain frequencies within the diurnal band. (Although our analysis deals with first mode diurnal shelf waves, the results are equally applicable to waves of other frequencies and modes provided the wavelengths can be assumed to vary much more rapidly than the alongshore changes in depth.) The forcing term $v_0(y, t)$ in (3.13) is considered to have the form

$$v_0(y, t) = A \cos(ky - \omega t), \quad (4.1)$$

corresponding to a barotropic Kelvin wave of frequency ω and wavenumber k traveling along the oceanic boundary. Although the amplitude for these waves has the general form $A \sim \exp(kx)$, it is sufficient for present purposes to take A = constant since the e-folding scale $k^{-1} = (gH)^{1/2}f^{-1}$ greatly exceeds the shelf width $L(k^{-1} > 15 \times 10^5$ m; $L < 1 \times 10^5$ m).

Substituting (4.1) into (3.13) yields

$$\Psi_{01}(y, t) = -E^{1/2}A(\omega/f)H_0 b_1 \times \int_{y_0}^{y} \cos[k\eta - \omega(s + t)]d\eta. \quad (4.2)$$

Integration then gives the alongshore component of the streamfunction

$$\Psi_{01}(y, t) = -E^{1/2} \frac{\omega H_0 b_1}{f(k - k_{01})} A \times \left[\sin(ky - \omega t) - \sin\left(ky_0 + \int_{y_0}^{y} k_{01}d\eta - \omega t\right)\right]; \quad (4.3)$$

this may also be written in the form of a spatially modulated traveling wave as

$$\Psi_{01}(y, t) = -E^{1/2} \frac{2\omega H_0 b_1}{f(k - k_{01})} \times A\sin\left[\tfrac{1}{2}k(y - y_0) - \tfrac{1}{2}\int_{y_0}^{y} k_{01}d\eta\right] \times \cos\left[\tfrac{1}{2}k(y - y_0) + \tfrac{1}{2}\int_{y_0}^{y} k_{01}d\eta - \omega t\right], \quad (4.4)$$

where

$$k_{01}(y) = \omega/c_{01}. \quad (4.5)$$

According to the above results, the response occurs at the forcing frequency ω and consists of two types of waves: a progressive, forced wave whose wavenumber k and phase speed ω/k match those of the Kelvin wave forcing (4.1); and a free, first mode continental shelf wave whose wavenumber k_{01} and phase speed ω/k_{01} are determined by the bottom topography through the eigenvalues to (3.5). The properties of these waves are allowed to vary alongshore in accordance with slow, $O(\epsilon^2)$, alongshore changes in depth. In theory, resonance solutions to (4.3) and (4.4) are possible when the phase speed of the shelf

waves is comparable to the phase speed of the Kelvin wave (i.e., $k_{01} \rightarrow k$). Eq. (4.4) then becomes

$$\Psi_{01} = -E^{1/2}(\omega/f)H_0 b_1(y - y_0) \times A\cos[k(y + y_0) - \omega t]$$

and the solution amplifies linearly with distance from the starting position $y = y_0$. However, in the particular case of diurnal shelf waves, phase speeds c_{01} are invariably small compared to the speed $(gH)^{1/2}$ of the barotropic tide so solutions are far removed from resonant conditions. Off the west coast of Vancouver Island, for example $(gH)^{1/2} \approx 200$ m s^{-1}, whereas calculated first mode shelf wave speeds are typically a few meters per second.

For relatively high frequency (i.e., diurnal) shelf waves are forced by diurnal tidal flows $k \ll k_{01}$ so that (4.4) takes the simplified form

$$\Psi_{01}(y, t) = -E^{1/2}\frac{2\omega H_0 b_1}{f k_{01}} A \sin\left(\frac{1}{2}\int_{y_0}^{y} k_{01} d\eta\right) \times \cos\left(\frac{1}{2}\int_{y_0}^{y} k_{01} d\eta - \omega t\right). \quad (4.6)$$

An identical solution is obtained from (4.1) and (4.2) by initially setting $k \equiv 0$, corresponding to a spatially uniform, time-varying tidal current. Such a model is locally valid in the sense that over a distance of one wavelength of a diurnal shelf wave (<500 km) the phase difference of a diurnal Kelvin wave is generally less than 15°. [Diurnal tides off the west coast of British Columbia have alongshore wavenumbers of ~2.4° (100 km)$^{-1}$.] Results similar to (4.6) have been derived by Adams and Buchwald (1969) and by Gill and Schumann (1974) for square wave wind stress forcing for the case k_{01} = constant. As shown in Fig. 2, the simplified solution for $y_0 = 0$ and constant k_{01} represents a spatially modulated progressive wave with nodal points fixed at integer multiples of the wavelength $(=2\pi k_{01}^{-1})$ from the starting point.

b. *Currents and sea surface elevations*

The zeroth order velocity components (u_1, v_1) of the forced first mode shelf wave are obtained using (4.6) and the solution to (3.5) in (3.3), together with (2.5). In particular

$$u_1 = H^{-1}\phi_1\Psi_{01,y}, \quad v_1 = -H^{-1}\phi_{1,x}\Psi_{01}, \quad (4.7)$$

where partial differentiation with respect to y must accommodate changes over both the fast (y) and slow $(\tilde{y})$ variables. When written in full (4.7) has the forms

$$u_1(x, y, t) = -(H_0/H)\phi_1 \tfrac{1}{2} k_{01}\beta_1 \times \cos\left(\int_{y_0}^{y} k_{01} d\eta - \omega t\right), \quad (4.8)$$

$$v_1(x, y, t) = (H_0/H)\beta_1\phi_{1,x}\sin\left(\frac{1}{2}\int_{y_0}^{y} k_{01} d\eta\right) \times \cos\left(\frac{1}{2}\int_{y_0}^{y} k_{01} d\eta - \omega t\right), \quad (4.9)$$

in which

$$\beta_1(\tilde{y}) = E^{1/2}(2\omega/f)A k_{01}^{-1} b_1. \quad (4.10)$$

A corresponding expression for the sea-surface slope is obtained by assuming a quasi-geostrophic balance in (2.2) whereby

$$fV \approx g\eta_x.$$

Substituting from (2.5) and integrating with respect

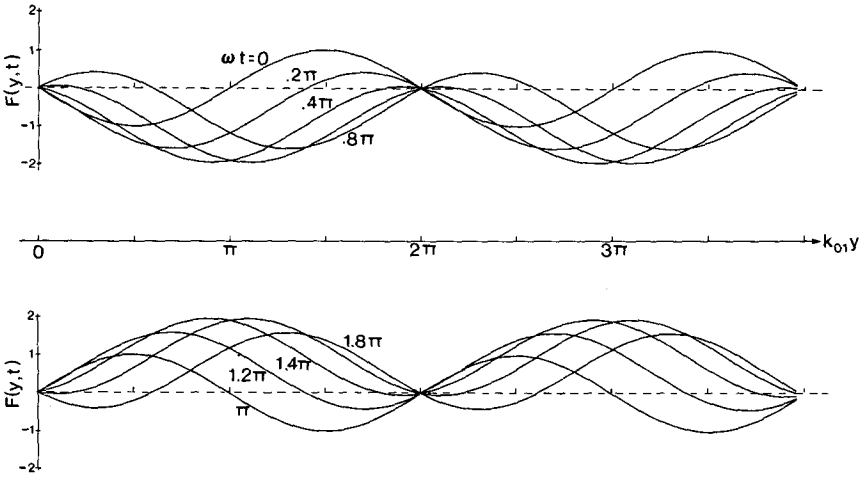

FIG. 2. Plots of $F(y, t) = \sin(\tfrac{1}{2}k_{01}y)\cos(\tfrac{1}{2}k_{01}y - \omega t)$ for $\omega t = 0, 0.2\pi, \ldots$. The function F corresponds to normalized streamfunction component Ψ_{01} and to normalized alongshore component $A^{-1}v_1$ of the shelf wave current for the case $y_0 = 0$ and k_{01} = constant.

TABLE 1. Normalized alongshore component of the mode 1 shelf wave velocity, $A^{-1}v_1'(x, y)$, at the coast ($x = 0$) at positions of maximum amplitude $y = (2m + 1)k_{01}^{-1}\pi$, $m = 0, 1, 2\cdots$, for the case $y_0 = 0$ and k_{01} = constant [cf Eq. (5.7)]. The depth $H(-L)$ = 2000 m is appropriate to the coast of Vancouver Island and A is the alongshore component of the Kelvin wave velocity; $\omega = 7.0 \times 10^{-5}$ s^{-1}; $f = 1.1 \times 10^{-4}$ s^{-1}.

μ (m^2 s^{-1})	H_0 (m)	l_1L	$-A^{-1}v_1'(0, y)$	μ (m^2 s^{-1})	H_0 (m)	l_1L	$-A^{-1}v_1'(0, y)$
10^{-4}	50	$\pi/2$	0.01	10^{-2}	50	$\pi/2$	0.10
10^{-4}	25	$\pi/2$	0.02	10^{-2}	25	$\pi/2$	0.15
10^{-4}	50	π	0.01	10^{-2}	50	π	0.14
10^{-4}	25	π	0.03	10^{-2}	25	π	0.27
10^{-4}	1	π	0.41	10^{-2}	1	π	4.13

to x yields

$$\eta_1(x, y, t) - \eta_1(-L, y, t) = (f/g)\int_{-L}^{x} v_1(x', y, t)dx', \quad (4.11)$$

as the onshore differences in sea level due to the presence of first mode shelf waves. Note that the alongshore amplitude and phase structure of (4.11) is identical to that of (4.9).

According to (4.9) and (4.11), the alongshore velocity component and cross-shelf sea surface slope attain maximum amplitudes at

$$y = (2m + 1)k_{01}^{-1}\pi, \quad m = 0, 1, 2, \cdots \quad (4.12)$$

from the starting point $y_0 = 0$ when $k_{01} \approx$ constant. The phases of these quantities differ from the phase of the tidal current forcing by

$$\Delta\theta = \pm\tfrac{1}{2}k_{01}\Delta s_m, \quad (4.13)$$

where Δs_m is the distance alongshore from a nodal point $y = 2mk_{01}^{-1}\pi$ (see Fig. 2). For $\Delta s_m > 0$, the sign of $\Delta\theta$ depends on the sign of $b_1\phi_{1,x}$. Where the latter is positive, the alongshore shelf wave current v_1 lags the alongshore tidal current v_0 from 180° to 0° over a distance of one wavelength in the direction of phase propagation; where it is negative, v_1 leads the tidal current from 180° to 0° over a wavelength. At mid-wavelength positions [(4.12)], the alongshore components of the shelf and Kelvin waves are 90° out of phase. When $b_1\phi_1 > 0$, the phase lag of the cross-shore component u_1 (4.8) relative to v_0 varies from 180° to 0° for $k_{01}y \leq \pi$ and from 0° to 180° for $k_{01}y \geq \pi$ over one wavelength. When $b_1\phi_1 < 0$, u_1 lags v_0 by 0° to 180° for $k_{01}y \leq \pi$ and by 180° to 0° for $k_{01}y \geq \pi$ over a wavelength. For most shelf regions, ϕ_1 and $\phi_{1,x}$ are of opposite sign.

5. Quantitative estimates

In this section we present some estimates of shelf wave current speeds and sea surface slopes. A convenient depth model for this purpose is the exponential profile

$$H(x) = \begin{cases} H_0e^{-2\alpha x}, & -L \leq x \leq 0 \\ H_0e^{2\alpha L}, & x \leq -L \end{cases} \quad (5.1)$$

where H_0, α and L can be treated as slowly varying functions of alongshore position. For the following calculations, however, constant values suffice.

Over the shelf-slope region, the eigenfunctions in (3.5) are for this model

$$\phi_n = a_ne^{-\alpha x}\sin(l_nx), \quad (5.2)$$

where, from boundary condition (3.6b),

$$\alpha \sin l_nL + l_n \cos l_nL = 0. \quad (5.3)$$

The wavenumber l_n in these expressions is related to the phase speed c_{0n} by

$$c_{0n} = 2\alpha f(l_n^2 + \alpha^2)^{-1}. \quad (5.4)$$

Using (5.1)–(5.3) in (3.10) we obtain

$$b_n = -2a_n\alpha l_nH_0^{-1}(l_n^2 + \alpha^2)^{-1} \leq 0, \quad (5.5)$$

which determines b_1 in (4.10). The coefficient a_n found from (5.1)–(5.3) and the normalization (3.9) is

$$a_n^2 = \frac{H_0}{\alpha[L + (\alpha/l_n^2)\sin^2 l_nL]}, \quad (5.6)$$

where we take the positive root.

Based on the above coefficients, it is straightforward to obtain estimates for the current speeds and surface elevations derived in Section 4. For example, with $y_0 = 0$ the alongshore velocity component (4.9) has a nearshore ($x \approx 0$) amplitude

$$v_1'(0, y) \approx \beta_1a_1l_1 \sin(\tfrac{1}{2}k_{01}y),$$

which, using (5.4)–(5.6) and the fact that $k_{0n} = \omega/c_{0n}$, can be written in expanded normalized form as

$$A^{-1}v_1'(0, y) \approx -8E^{1/2}G(l_1, \alpha)\sin(\tfrac{1}{2}k_{01}y), \quad (5.7)$$

where A is the tidal current amplitude, $E = \mu \times (2\omega H_0^2)^{-1}$ by (2.10), and

$$G(l_1, \alpha) \equiv (l_1\alpha)^2(l_1^2 + \alpha^2)^{-2} \times [\alpha L + (\alpha^2/l_1^2)\sin^2 l_1L]^{-1}. \quad (5.8)$$

Estimates for (5.7) at positions (4.12) are presented in Table 1 for various values of l_1, H_0 and μ. To construct this table we have used the fact that l_n in

(5.3) satisfies

$$(n - \tfrac{1}{2})\pi \leqslant l_n L \leqslant n\pi \tag{5.8}$$

(Adams and Buchwald, 1969) and have considered only the extreme values $l_1 L = \pi, \tfrac{1}{2}\pi$. Moreover from (5.1) we have

$$\alpha L = \tfrac{1}{2} \ln[H(-L)/H_0], \tag{5.9}$$

so that all parameters in (5.7) except μ and l_1 are determined once $H(-L)$ and H_0 are specified. The number obtained for the ratio (5.7) is therefore strongly dependent on the values chosen for the shore depth H_0 and the eddy viscosity μ. Though both are ambiguous, we could expect the range

$$10^{-4} < \mu < 10^{-2} \text{ m}^2 \text{ s}^{-1} \tag{5.10}$$

to be representative of weak to strong turbulent motions in the bottom boundary layer. The scale depth H_0 which most closely models the shelf-slope region seaward of the coast of Vancouver Island is in the range 25–50 m while values of 25–100 m are typical of shelf regions in general. The unphysical case $H_0 = 1$ m is included here to indicate the extreme amplification predicted by the theory. For a monotonically increasing depth away from shore, the velocity component v_1 will be a maximum at the coast. The cross-shelf component u_1 is zero at the coast and reaches maximum amplitude near the shelf break.

The cross-shelf difference in sea-surface elevation due to first mode shelf waves can be derived from (4.9) and (4.11). If we disregard the time-dependent factor, the magnitude of the elevation difference between the coast and the outer shelf, defined by $\Delta\eta = \eta_1(0, y) - \eta_1(-L, y)$, is given by

$$\Delta\eta = -(f/g)\beta_1 a_1 F(l_1, \alpha) \sin(\tfrac{1}{2}k_{01}y), \tag{5.11}$$

where we have used (5.1) and (5.2) in the integration and where

$$F(l_1, \alpha) \equiv (\alpha/l_1)(1 - e^{-\alpha L} \cos l_1 L) + \frac{l_1^2 - \alpha^2}{l_1^2 + \alpha^2} e^{-\alpha L}[\sin l_1 L + (\alpha/l_1) \cos l_1 L].$$

Estimates of the nondimensionalized height difference $l_1\Delta\eta$ are presented in Table 2 for a tidal current speed of 1 cm s^{-1}. To obtain the appropriate dimensional quantities, we multiply by L and use the specified value $l_1 L$. For example, for the case $l_1 L = \pi/2$, $\mu = 10^{-2}$ m^{-2} s^{-1} and $\alpha L = 2.19$ corresponding to $H_0 = 25$ m and $H(-L) = 2000$ m, we find $l_1\Delta\eta = 2.01 \times 10^{-8}$. Hence for a shelf width L of 100 km and a tidal current of 1 cm s^{-1}, we obtain

$$\Delta\eta \approx 1.3 \text{ mm},$$

which is a small but acceptable value for these long, nondivergent wave motions. Again, the magnitude of the estimate for this particular depth model is increased for smaller H_0 or for larger friction and tidal current speed.

TABLE 2. Differences in cross-shelf sea-surface elevations $\Delta\eta$ between the coast ($x = 0$) and the shelf edge ($x = -L$) for mode 1 shelf waves at $y = (2m + 1)k_{01}^{-1}\pi$ for the case $y_0 = 0$ and k_{01} = constant [cf. Eq. (5.11)]. To obtain $\Delta\eta$ for given shelf width, multiply by L and use appropriate value of $l_1 L$. $\omega = 7.0 \times 10^{-5}$ s^{-1}; $f = 1.1 \times 10^{-4}$ s^{-1}; $g = 9.8$ m s^{-2}; $H(-L) = 2000$ m; and $L = 10^2$ km. Height difference is proportional to A which has been set at 1 cm s^{-1}.

μ (m^2 s^{-1})	H_0 (m)	$l_1 L$	$l_1\Delta\eta$ ($\times 10^{-8}$)	$\Delta\eta$ (mm)
10^{-4}	50	$\pi/2$	0.13	0.08
10^{-4}	25	π	0.23	0.07
10^{-2}	50	$\pi/2$	1.33	0.85
10^{-2}	25	$\pi/2$	2.01	1.28
10^{-2}	1	π	59.10	18.80

The phases of the currents are also readily obtained for the exponential shelf profile. In particular, we find $\beta_1\phi_1 \geqslant 0$ in (4.8), based on (5.8), and $\beta_1\phi_{1,x} \leqslant 0$ in (4.9) except perhaps for the outer portion of the slope where $\phi_{1,x}$ changes sign. Near the starting location $y \approx y_0$, for example, both u_1 and v_1 will be 180° out of phase with v_0 but will alter their phase for increasing distance from this location. Furthermore, the velocity vector (u_1, v_1) at a given position rotates clockwise with time over the shelf and traces out an ellipse with major-to-minor axis ratio $|v_1|/|u_1|$.

6. Discussion and summary

In this paper, we have presented an idealized model for tidally forced continental shelf waves that neglects the effects of advection, friction, nonlinearity and stratification on the wave properties. Moreover, the governing vorticity equation for the model is based on an expansion variable which, though less than unity, is not strictly small for the main frequencies of interest. Despite such limitations, the theory appears to account for many features of diurnal shelf waves.

Shelf waves generated through subinertial tidal oscillations are expected to be predominantly of K_1 and O_1 frequency since these usually are the major diurnal tidal frequencies. Presumably, the amplitude and phases of these waves also vary in concert with the fortnightly and longer variations in the tides. However, unlike the low-frequency coastal oscillations produced by transient wind systems, the tidally forced shelf waves are not expected to have widespread global distribution. Such waves are not only confined to latitudes poleward of 30° and to regions with significant diurnal tidal currents, but they are also restricted to sections of continental margins whose bathymetry is able to support high-frequency shelf wave motions. Where they can exist, the waves will be permanent features of the coastal environment.

Based on experience with actual shelf-slope topography, we expect barotropic diurnal shelf waves to consist of first mode oscillations only. In that case, the relatively long-wavelength, low-frequency (0.0387 cph) O_1 oscillations should appear first on a section of a coast where the depth $H(x, y)$ first begins to permit shelf waves of diurnal period. Strictly speaking, both the amplitude and group velocity of the waves are zero at this location, although in reality there will be a nonzero energy flux within a finite region about the bathymetric transition zone. The O_1 shelf waves generated along the extent of the coastal region will consist of long waves with group velocity $\mathbf{c}_g$ in the direction of the phase velocity $\mathbf{c}$ and/or short waves with $\mathbf{c}_g$ in the opposite direction to $\mathbf{c}$. Since they have greater phase speeds and considerably longer wavelengths, the former are less subject to frictional and nonlinear effects and are therefore expected to prevail. Moreover, the stratification tends to eliminate the shorter of the two waves for fixed frequency (Huthnance, 1978).

Provided the slowly changing topography continues to allow for an increase alongshore in the maximum permissible wave frequency, K_1 (0.0418 cph) shelf waves should next appear within the shelf-slope region. The starting location for these higher frequency waves is therefore displaced alongshore from that of the O_1 shelf waves. Again, the longer waves are expected to predominate. The wavenumbers and amplitudes of both the O_1 and K_1 waves will be modulated by the slowly varying bathymetry and their alongshore velocity components will attain maximum speeds roughly midway between the fixed nodal points $y = 2mk_{01}^{-1}\pi$. In general, the alongshore currents of the two shelf waves should be maximum at separate locations along the coast. However, the fact that K_1 waves are significantly shorter than the O_1 waves and initially begin further along the coast, indicates that at certain locations the maxima could coincide.

If we assume that $b_1 \leqslant 0$ and $\phi_{1,x} \geqslant 0$, as suggested by the results of Section 5, then the alongshore current v_1 and sea surface elevation η_1 will consistently lead in phase the alongshore component of the tidal current, v_0 and local tide height, respectively. Near the starting point for a particular frequency, v_1 will lead v_0 by 180°; at the midway position where v_1 is maximum, v_1 will lead by 90°; and immediately before the next alongshore nodal location, the two will have approximately equal phases. Consequently, there is a discontinuity in phase at each nodal position, from 0° to 180° in the direction of phase propagation (cf. Fig. 2). The cross-shelf velocity component u_1 has the form of a propagating wave whose phase relative to the tidal forcing varies as $k_{01}y$. Shelf wave currents at the nodal points of v_1 therefore consist of an on-offshore flow only. In addition to the u, v components, the shelf wave current for a given tidal constituent can be expressed in terms of counter-rotating polarized vectors. Fig. 3 shows the orientation of the predominant clockwise component of the shelf wave current as a function of position along the coast at the time of maximum tidal current, or roughly the time of high water at the shore. This component is found here by setting $k_{01}\phi_1$ equal to $\phi_{1,x}$ and plotting the phase of the total current using (4.8) and (4.9) for the case $\omega t = 0$ and k_{01} = constant. The vector is seen to rotate in a counterclockwise sense with y in the direction of phase propagation and completes a 360° turn in one wavelength of the shelf wave. Where k_{01} is a slowly varying function of y, the orientation angle of the clockwise current vector will not increase uniformly with y as in Fig. 3 but will vary as $\int_{y_0}^{y} k_{01}dy'$ from the start position y_0.

Two other points are noted here. First, the group velocity of a first mode wave is nearly zero in the vicinity of the starting location. This is because the peak frequency in the dispersion curve $\omega(k)$ is also the frequency for which $|\mathbf{c}_g| = \partial\omega/\partial k = 0$. As a consequence, energy will leak slowly away from such regions, leading to the possibility of resonant amplification of the shelf waves. If such resonance is indeed important to the overall growth of the waves, the K_1 shelf waves will be amplified more than the O_1 waves owing to the former's closer proximity to the wavenumbers for zero group velocity. This would account for the observation that K_1 shelf waves are amplified more than O_1 shelf waves relative to their respective tidal currents (Cartwright, 1969).

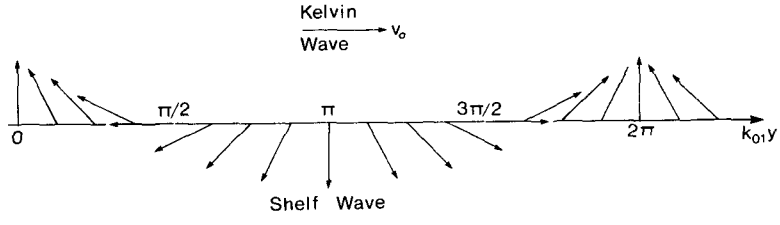

FIG. 3. Variation alongshore in the orientation of the clockwise rotating vector component of the first mode shelf wave current (u_1, v_1) over the continental shelf for constant wavenumber at times of maximum tidal current; $\omega t = 0, 2\pi, \cdots$ in (4.1). The amplitude of each vector is determined once ϕ_1, $\phi_{1,x}$ and k_{01} are specified as functions of x and y.

The other point is that somewhere along a given coast, in the direction of phase propagation, the waves will encounter a second depth transition region beyond which the topography will no longer support the diurnal period oscillations. Because we are assuming slow alongshore variations in depth, we expect the waves to propagate into this region and decay, with a minimal amount of energy reflection taking place at the transition zone. However, more abrupt transitions could cause a significant percentage of the energy to be reflected as shorter waves with oppositely directed group velocity to the longer incident waves.

Generation mechanism

The way in which the tidal oscillations generate shelf waves is analogous to the process described by Gill and Schumann (1974). To begin with, the tidal flow over the bottom produces a frictional Stokes-scale boundary layer with a time-dependent, alongshore Reynolds stress component, $-\tau^{(y)}/H$. This stress, combined with the Coriolis effect, leads to a cross-shelf mass flux within the bottom boundary layer. Since there can be no net transport at the coastal boundary and since the response is essentially non-divergent, the mass flux in the boundary layer must be compensated by a mass flux within the bulk of the overlying fluid. This leads, in turn, to onshore-offshore displacements at tidal frequencies of water columns and a corresponding shrinking and stretching of vortex lines f/H. Where the topography can act as a horizontal restoring mechanism for these displacements, the tidal motions are able to efficiently "pump" energy into the shelf wave motions. The fact that the amplitude of the streamfunction is strongly modulated alongshore, with nodal points at intervals of a wavelength, is due to the interference between the locally generated wave and free waves propagating into the region from adjoining coastal sections. Nodal locations are points of total destructive interference.

Lastly we note that, although the generation mechanism is probably inefficient because of the short time allowed for establishment of the bottom boundary layer over each half-tidal cycle, this is presumably compensated by the small group velocities, especially for the K_1 waves, and by the fact that tidally-induced turbulent motions are always present.

Acknowledgments. We wish to thank Roger Grimshaw, Paul LeBlond and Lawrence Mysak for their helpful suggestions and discussions during the development of this work. We also thank David Ramsden and Liliane Kuwahara for assistance with the figures and Billie Mathias for typing the manuscript.

REFERENCES

Adams, J. K., and V. T. Buchwald, 1969: The generation of continental shelf waves. *J. Fluid Mech.*, **35,** 815–826.

Allen, J. S., 1980: Models of wind-driven currents on the continental shelf. *Annual Review of Fluid Mechanics*, Vol. 12, Annual Reviews, Inc., 389–433.

Batchelor, G. K., 1967: *An Introduction to Fluid Dynamics*. Cambridge University Press, 615 pp.

Cartwright, D. E., 1969: Extraordinary tidal currents near St. Kilda. *Nature*, **233,** 928–932.

——, J. M. Huthnance, R. Spencer and J. M. Vassie, 1980: On the St. Kilda shelf tidal regime. *Deep-Sea Res.*, **27A,** 61–70.

Crawford, W. R., and R. E. Thomson, 1982: Continental shelf waves of diurnal period along Vancouver Island. *J. Geophys. Res.* (in press).

Gill, A. E., and E. H. Schumann, 1974: The generation of long shelf waves by the wind. *J. Phys. Oceanogr.*, **4,** 83–90.

Huthnance, J. M., 1978: On coastal trapped waves: Analysis and numerical calculation by inverse interation. *J. Phys. Oceanogr.*, **8,** 74–92.

——, 1981: Waves and currents near the continental shelf edge. *Prog. Oceanogr.*, **10,** 193–226.

LeBlond, P. H., and L. A. Mysak, 1978: *Waves in the Ocean*. Elsevier Scientific, 602 pp.

Morse, P. M., and H. Feshbach, 1953: *Methods of Theoretical Physics*, Vol. 1. McGraw-Hill, 997 pp.

Mysak, L. A., 1980: Recent advances in shelf wave dynamics. *Rev. Geophys. Space Phys.*, **18,** 211–241.

Thomson, R. E., and W. S. Huggett, 1981: Wind generated inertial oscillations of large spatial coherence. *Atmos.-Ocean*, **19,** 281–306.